

---

# Benchmarking Deep Inverse Models over time, and the Neural-Adjoint method

---

**Simiao Ren**

Dept. of Electrical and Computer Engineering  
Duke University  
Durham, NC 27705  
simiao.ren@duke.edu

**Willie Padilla**

Dept. of Electrical and Computer Engineering  
Duke University  
Durham, NC 27705  
willie.padilla@duke.edu

**Jordan Malof**

Dept. of Electrical and Computer Engineering  
Duke University  
Durham, NC 27705  
jordan.malof@duke.edu

## Abstract

We consider the task of solving generic inverse problems, where one wishes to determine the hidden parameters of a natural system that will give rise to a particular set of measurements. Recently many new approaches based upon deep learning have arisen generating impressive results. We conceptualize these models as different schemes for efficiently, but randomly, exploring the space of possible inverse solutions. As a result, the accuracy of each approach should be evaluated as a function of time rather than a single estimated solution, as is often done now. Using this metric, we compare several state-of-the-art inverse modeling approaches on four benchmark tasks: two existing tasks, one simple task for visualization and one new task from metamaterial design. Finally, inspired by our conception of the inverse problem, we explore a solution that uses a deep learning model to approximate the forward model, and then uses backpropagation to search for good inverse solutions. This approach, termed the neural-adjoint, achieves the best performance in many scenarios.

## 1 Introduction

In this work we consider the task of solving generic inverse problems. An inverse problem is characterized by a forward problem that models, for example, a real-world measurement process or an auxiliary prediction task. The forward problem can be written as

$$y = f(x) \tag{1}$$

where  $y$  is the measurable data,  $f$  is a (non-)linear forward operator that models the measurement process, and  $x$  is an unobserved signal of interest. Given  $f$ , solving the inverse problem is then a matter of finding an inverse model  $x = f^{-1}(y)$ . However, if the problem is ill-posed or the forward problem is non-linear, finding  $f^{-1}$  is a non-trivial task. Specific inverse problems can be solved using apriori knowledge about  $f$ , (e.g., sparsity in some basis, such as compressed sensing), however, we consider the task of solving generic inverse problems, where no such solutions are known.

Recently many new approaches based upon deep learning have arisen, generating impressive results. These methods typically require a dataset of sample pairs  $\{x_n, y_n\}_{n=1}^N$  from  $f$ , from which a deep

neural network model can be trained to approximate the inverse model,  $\hat{f}^{-1}$ . Some recent examples include models based on normalizing flows (e.g., invertible neural networks [1, 2]), variational auto-encoders [3], and tandem architectures [4, 5].

### 1.1 Modern inverse models as stochastic search

Despite the apparent variety of recent approaches, most of these inverse models can be written in the form  $\hat{x} = \hat{f}^{-1}(y, z)$ , where  $z$  is randomly drawn from some probabilistic distribution  $Z$  (e.g., Gaussian)[1]. Although the interpretation of  $z$  varies across these models, they all share the property that  $\hat{x}$  will vary depending upon the value of  $z$ . Furthermore, since it is usually trivial and fast to evaluate the accuracy of candidate solutions using the forward model (or an approximation of it), one can sample multiple values of  $z$  in search of more accurate solutions. Therefore, each inverse model can be viewed as a means of efficiently, but nonetheless stochastically, searching through  $x$ -space for good inverse solutions. In section 6.2 we visualize this search process for several models as a function of  $z$ .

From this perspective, the performance of each inverse model is dependent upon the number of  $z$  samples that are considered, denoted  $T$ . For example, one model may perform best when  $T = 1$ , while another model performs best as  $T$  grows. Our experiments here show that this is indeed the case, and model performance is highly dependent upon  $T$ . Typically however the performance,  $r$ , of an inverse models is judged by estimating its expected,  $E$ , "re-simulation" error [2] over the data latent variable distributions, denoted  $D$  and  $Z$  respectively. Mathematically, we have

$$r = E_{(x,y) \sim D, z \sim Z} [\mathcal{L}(\hat{y}(z), y)] \quad (2)$$

where  $\hat{y}(z) = f(\hat{f}^{-1}(y, z))$  is the "re-simulated" value of  $y$  produced by passing  $\hat{x}$  (an estimate) through the forward model, and  $\mathcal{L}$  is the user-chosen loss function (e.g., L2 loss). The metric  $r$  effectively measures error under the assumption we always utilize one sample of  $z$  (given a target  $y$ ). Here we propose an alternative metric that quantifies the expected *minimum* error if we draw a sequence of  $z$  values of length  $T$ , denoted  $Z_T$ . Formally, this is given by

$$r_T = E_{(x,y) \sim D, Z_T \sim \Omega} \left[ \min_{z \in Z_T} [\mathcal{L}(\hat{y}(z), y)] \right] \quad (3)$$

where  $Z_T$  is a sequence of length  $T$  drawn from a distribution  $\Omega$ . This measure characterizes the expected loss of an inverse model *as a function of* the number of samples of  $z$  we can consider for each target  $y$ . In this work we conduct a benchmark study of four tasks with  $r_T$ , and we find that the performance of modern inverse models depend strongly on  $T$ , revealing the limitation of existing metrics, and revealing useful insights about the way in which each model searches  $x$ -space. In particular, we present analysis suggesting that modern inverse models suffer from one or both of the following limitations: (i) they don't fully explore  $x$ -space, missing some solutions; or (ii) they do not precisely localize the optimal solutions, introducing errors.

### 1.2 The neural-adjoint method

Motivated by the weaknesses of existing methods, we develop the Neural-Adjoint (NA), inspired by the classical Adjoint approach for inverse design problems[6, 7]. The main idea is to train a neural network to approximate  $f$  and then, starting from different random locations in  $x$ -space, use  $\partial \hat{f} / \partial x$  descend towards locally optimal  $x$  values. Surprisingly, this simple approach almost always yields the lowest error among all models, tasks and  $T$ -values considered in our benchmarks. Our analysis suggests that, in contrast to other models, NA fully explores the  $x$ -space, and also accurately localizes inverse solutions. NA achieves this advantage at the cost of significantly higher computation time, although as we discuss, this is only problematic for especially time-sensitive applications.

We next summarize the three primary contributions of this work:

1. *A comprehensive benchmark comparison using  $r_T$ .* We compare five modern inverse models on four benchmark tasks. The results reveal the performance of modern models under many different conditions. Using  $r_T$  we reveal that the accuracy of modern models depends strongly on  $T$ .
2. *A new modern benchmark task, and a general method to replicate it.* We introduce a contemporary and challenging inverse problem for meta-material design. Normally, it would

be difficult for others to replicate our studies because requires sophisticated electromagnetic simulations. However, we introduce a strategy for creating simple, fast, and sharable *approximate* simulators for complex problems, permitting easy replication.

3. *The neural-adjoint method.* We develop the NA method, which nearly always outperforms all other models we consider in our benchmark. Furthermore, our analysis provides insights about the limitations of existing models, and why NA is so effective.

We release code for all inverse models, as well as (fast) simulation software for each benchmark problem, so that other researchers can easily repeat our experiments.

## 2 Related Work

**Modern deep inverse models.** Direct learning of the one-to-many inverse relationship is intractable even for trivial tasks, [8] and various architectures have been proposed as potential solutions. For example, one problem caused by one-to-many inverse mapping is gradient instability due to data collision. To address this inconsistent gradient information, cyclic consistent loss or Tandem models [4, 9, 10, 11] have proven their ability to avoid this dilemma by connecting a forward model to the backward model, thereby suppressing gradient feedback due to different correct answers. An alternative approach is to model the conditional posterior directly using variational methods [12, 13]. Variational Auto-Encoders [3] consist of an encoder and decoder, and model the joint distribution of hidden and measurement states, to normal distributions  $z$ , and decode inverse solutions from samples. By minimizing the evidence lower bound, it trades between reconstruction accuracy and transformed joint distribution closeness to normal distribution. Earlier work on Mixture density networks [14] model the direct conditional distribution using gaussians. However due to low accuracy reported by [2], we do not include comparison to this work. With recent advance in the normalizing flow community [15, 16, 17, 18, 19, 20], Ardizzone [1] first applied a state-of-the-art invertible neural network to the inverse problem. Utilizing various invertible network-based architectures, Kruse [2] benchmarked them on two simple inverse problems. It was found that conditional invertible networks, and invertible networks trained by maximum likelihood, had the best performance; we thus select these winners to compare further with other methods.

**Inverse model performance metrics.** Although the architecture varies across different studies, the performance metric used in each is largely identical. Nearly all the studies on inverse regression problems uses either Mean Squared Error or Root Mean Squared Error *with only one evaluation*, [1, 2, 4, 8, 11, 12, 13, 21] despite the stochastic nature of some approaches, which can produce different solutions for the same target.

**The Adjoint method.** The adjoint method is a popular approach in control theory or engineering design that calculate the gradient from end measurement parameter to controllable parameters and use that gradient information to guide better design. The NA method proposed also utilizes gradients of the forward model to identify locally optimal inverse solutions. However, by using a neural network to approximate the forward model (and its gradients) there is no need to derive an analytic gradient. We were also inspired to explore this general strategy by recent work in [21] where success on a single problem using a similar concept. We build on their work by (i) developing a detailed description of the methodology, (ii) introducing two innovations (boundary loss and sampling design) that improve the accuracy and reliability of the approach, and (iii) conducting a comprehensive comparison of the resulting approach (NA) against modern models.

## 3 The Neural-Adjoint Method

The NA method can be divided into two steps: (i) Training a neural network approximation of  $f$ , and (ii) inference of  $\hat{x}$ . Step (i) is conventional and involves training a generic neural network on a dataset of input/output pairs from the simulator, denoted  $D$ , resulting in  $\hat{f}$ , an approximation of the forward model. This is illustrated in the left inset of Fig 1. In step (ii), our goal is to use  $\partial\hat{f}/\partial x$  to help us gradually adjust  $x$  so that we achieve a desired output of the forward model,  $y$ . This is similar to many classical inverse modeling approaches, such as the popular Adjoint method [6, 7]. For many practical inverse problems, however, obtaining  $\partial\hat{f}/\partial x$  requires significant expertise and/or effort, making these approaches challenging. Crucially,  $\hat{f}$  from step (i) provides us with a closed-form differentiable

expression for the simulator, from which it is trivial to compute  $\partial \hat{f} / \partial x$ , and furthermore, we can use modern deep learning software packages to efficiently estimate gradients, given a loss function  $\mathcal{L}$ .

More formally, let  $y$  be our target output, and let  $\hat{x}^i$  be our current estimate of the solution, where  $i$  indexes each solution we obtain in an iterative gradient-based estimation procedure. Then we compute  $\hat{x}^{i+1}$  with

$$\hat{x}^{i+1} = \hat{x}^i + \alpha \left. \frac{\partial \mathcal{L}(\hat{f}(\hat{x}^i), y)}{\partial x} \right|_{x=\hat{x}^i} \quad (4)$$

where  $\alpha$  is the learning rate, which can be made adaptive using conventional approaches like Adam [22]. Notice that the parameters of the neural network are *fixed*, and we are only adjusting the input to the network, treating them like model parameters. Our initial solution,  $\hat{x}^0$  is drawn from some distribution  $\Gamma$ .

Given some desired  $y$ , NA iteratively adjusts its estimated solution (beginning with  $\hat{x}_0$ ) until convergence (e.g.,  $\mathcal{L}$  no longer reduces). This entire process acts as the inverse model for the process,  $\hat{f}^{-1}(y, z)$ , where  $z = \hat{x}^0 \sim \Gamma$ . This is illustrated in the right inset of Fig 1. Similar to other approaches, we can draw a sequence of  $z$  values and obtain an estimated solution for each one. As we show in our experiments, the NA model is highly effective, because it is iterative it is also much more computationally expensive than other approaches.

### 3.1 Obtaining good results: designing $\Gamma$ , and the boundary loss

There are two crucial components needed to obtain good results with NA. The first component is an additional loss during inference that guides the network to choose solutions within the domain of the training data. We found that, without this addition, the NA would frequently converge to solutions that were outside of the training data distribution, resulting in both inaccurate and/or unrealistic solutions. This occurs because the  $\hat{f}$  becomes highly inaccurate outside of the training data domain, and (erroneously) predicts that  $x$ -values in this space will produce the desired  $y$  (or a close approximation). We hypothesize that the probability of seemingly good solutions increases outside of the training domain because  $\hat{f}$  behaves in a random and highly variable way. To discourage this behavior we add a simple “boundary loss” term (only during inference) that encourages NA to converge to solutions within the training data domain. This loss term, denoted  $\mathcal{L}_{bnd}$ , is given by

$$\mathcal{L}_{bnd} = ReLU(|\hat{x} - \mu_x| - 2\sigma_x) \quad (5)$$

where  $\mu_x$  is the mean of the training data,  $\sigma_x$  is its standard deviation, and ReLU is the conventional neural network activation function. We found that, without  $\mathcal{L}_{bnd}$ , the performance of NA would degrade severely, as shown by ablation studies in the supplement.

A second important component of NA is design of the sampling distribution,  $\Gamma$ , of  $\hat{x}_0$ . It may be intuitive to set  $\Gamma$  as a Gaussian or Uniform distribution however, we found the best results if  $\Gamma$  matched the  $x$  sampling distribution for each task. In our case, and in most practical settings, these distributions were known apriori, and so we set  $\Gamma$  using this knowledge. In the supplement we present ablation studies for this training strategy.

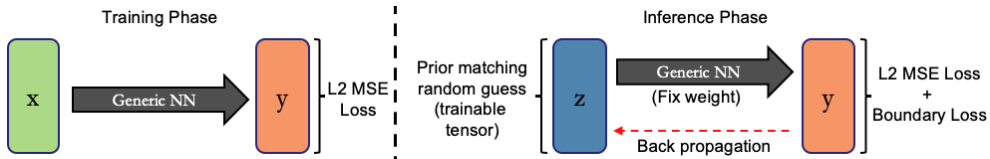


Figure 1: Architecture of Neural Adjoint method

## 4 Benchmark deep inverse models

In this section we briefly describe the inverse models that we employ in our benchmark experiments. We focus on the motivation and relevant properties of each model, however, much more detail for each model can be found in the supplement.

**Tandem model.** [4, 5] This is an encoder-decoder structure where the forward mapping  $\hat{f}$  (decoder) from  $x$  to  $y$  is trained first, after which its parameters are fixed and an inverse model (encoder) is pre-pended to the decoder and trained to solve the inverse mapping using end-to-end backpropagation over the whole model. Typically an L2 loss is used for training, but we found that adding in our boundary loss (see 3.1), so that the total loss for training is given by

$$Loss = (\hat{f}(\hat{x}) - y_{gt})^2 + ReLU(|\hat{x} - \mu_x| - 2\sigma_x) \quad (6)$$

In the supplement we provide ablation studies showing that adding the boundary loss is indeed beneficial for this approach. Once trained, the output of the Tandem model does not depend upon any stochastic input,  $z$ , and therefore its performance does not vary as a function of  $T$ . Except for the extra boundary loss, we used the implementation introduced by [4] for this approach.

**Conditional Variational Auto-Encoder (cVAE).** [12, 13] Created by Kingma [3] it encodes  $x$ , conditioned on  $y$ , into a Gaussian distributed random variable  $z$ . It is a bayesian approach with a prior loss of Evidence Lower Bound.

$$Loss = (x - \hat{x})^2 - \frac{\alpha}{2} \cdot (1 + \log\sigma_z + \mu_z^2 - \sigma_z) \quad (7)$$

$Z$  (re-parameterized into  $\sigma_z, \mu_z$ ) represents the transformed distribution of hidden state  $x$  given  $y$ . The transformation is learnt with trade-off between the reconstruction (decoding back to exactly the same  $x$ ) and distribution ( $z$  being normal). cVAE explores the solution space by drawing new examples from  $\sigma_z, \mu_z$ . We used the implementation introduced by [12] for this approach.

**Invertible Neural Networks (INN).** Invertible Neural Network, based upon the RealNVP [15], have recently shown great potential for solving various inverse problems [1]. To circumvent the one-to-many mapping problem, the network learns the bijective mapping between  $x$  and  $y \otimes z$  space by padding the "smaller" space  $y$  with some random number space  $z$ , hoping to learn different  $x$  that maps to the same  $y$  with an extra latent variable  $z$ . There are 2 ways of training reported in [2], one with supervised L2 loss combined with a distribution loss Maximum Mean Discrepancy (MMD) [23] and the other with simply maximum likelihood loss with normal distribution assumption [15]. Since the Maximum likelihood estimation (MLE) training gives a better solution in the literature, we are adopting the MLE training scheme here.

$$Loss = \frac{1}{2} \cdot \left( \frac{1}{\sigma^2} \cdot (\hat{y} - y_{gt})^2 + z^2 \right) - \log|\det J_{x \rightarrow [y,z]}| \quad (8)$$

where  $J$  means the Jacobian of mapping from  $x$  to  $y \otimes z$  space and  $z$  represents the transformed remnant distribution of  $x$  after having  $y$ . Exploration of the inverse solution space is similar with aforementioned cVAE where different  $z$  values are being input with the same  $y$  value. Note that the assumptions of this method make it inapplicable to problems where the output dimension is larger than the input dimension in forward mapping.

**Conditional Invertible Neural Networks (cINN).** Conditional INNs use a similar network structure as INNs, with a modification that instead of learning the bijective mapping from  $x$  to  $y \otimes z$  space, it learns the bijective relationship between  $x$  and  $z$  space under condition  $y$ . The network is trained under MLE loss as well, with the caveat that  $y$  does not appear in the loss function due to conditioning.

$$Loss = \frac{1}{2}z^2 - \log|\det J_{x \rightarrow z}| \quad (9)$$

Here  $z$  represents the full transformed distribution of  $x$  conditioned on  $y$ . Exploring inverse solution space also requires sampling different  $z$  values. We adopted the original author's implementation in both invertible networks, [2] in order to avoid inadvertent alteration of the comparison condition.

## 5 Benchmark Tasks

We consider four benchmark tasks, which are summarized in Table 1. Inspired by the recent benchmark study [2], we include two popular existing tasks: ballistics targeting (D1), and robotic arm control (D3). For these two tasks we use the same experimental designs as [2], including their simulator (i.e., forward model) parameters, simulator sampling procedures, and their training/testing splits. All details can be found in [2] and our supplement. The remaining two benchmarks are new, and we describe them next.

### 5.1 A new meta-material benchmark (D4), and a technique for replicating it

The goal of this task, recently posed in [24], is to design the radii and heights of four cylinders (i.e.,  $x \in \mathbb{R}^8$ ) of a meta-material so that it produces a desired electromagnetic (EM) reflection spectrum ( $y \in \mathbb{R}^{300}$ ), illustrated in Fig. 2. The input and output are (relatively) high-dimensional and non-linear, and  $f(x)$  can only be evaluated using a slow iterative EM simulators, requiring significant time and expertise. These challenges are typical of modern (meta-)material design problems, forming a major obstacle to progress. Substantial recent research has been conducted on similar problems (e.g., [12, 21, 4, 25, 26]), making this both a challenging and high-impact benchmark problem.

Problems like this are not suitable as benchmarks due to the computation time, needed domain expertise, and required use of a simulator. It is also insufficient simply to share data from the simulator, due to the need to draw new samples from  $f(x)$  when evaluating inverse models. We overcome this problem by generating a large number of samples from our simulator (approx. 40,000), and then training an ensemble of deep neural networks to approximate the simulator. This yields a highly accurate simulator (mean-squared-error of  $6e-5$ ) that is fast, portable, and easy to use by others. All of our experiments utilize data sampled from this proxy simulator rather than the original simulator. We hypothesized that the difficulty of our meta-material problem may be undermined because we use the same class of models (neural networks) for both the proxy-simulator and our inverse models. We mitigate this risk by providing a much larger set of training data to the simulator model, and using an ensemble of large and varying models (rather than one small model) for the proxy-simulator.

### 5.2 The 2-dimensional sinusoidal benchmark (D2)

This benchmark problem consists of a simple 2-dimensional sinusoidal function, of the following form:  $y = \sin(3\pi x_1) + \cos(3\pi x_2)$ . We included this problem because it had both of the following properties: (i) despite its simplicity, we found it is challenging for most of the deep inverse model; (ii) its 2-dimensional input space allowed us to visualize the solutions produced by each inverse model, and study the nature of their errors. We utilize these properties to gain deeper insights about the inverse models in Section 6.2.

Table 1: Benchmarking datasets outline

ID	Dataset	Dim(x)	Dim(y)
D1	Ballistics	4	1
D2	Sine wave	2	1
D3	Robotic arm	4	2
D4	Meta-material	8	300

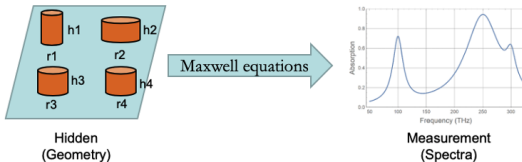


Figure 2: Illustration of the meta-material problem

## 6 Experimental Design and Results

We follow closely the design of the recent benchmark study [2]. For all experimental scenarios that we share with [2], we followed their design and obtained (with one exception) similar results. This includes results for the cINN, INN and cVAE models; on the Robotic Arm and Ballistics tasks. In an effort to compare models fairly, we constrained the newly included models - Tandem and NA - to have the same number (or less) of trainable parameters. Furthermore, all models utilized the same training and testing data, batch size, and stopping criteria (for training). In those cases where model hyperparameters were not available from [2], we budgeted approximately one day of computation time (on common hardware) to optimize hyperparameters, while again constraining model sizes. Full implementation details can be found in the supplementary material.

Once each model was trained, we estimated its error,  $r_T$  for  $T \in \{1, 10, 20, \dots, 50\}$  using  $D = \{x_n, y_n\}_{n=1}^N$  random samples from the simulator. We used the following sample estimator of  $r_T$ :

$$\hat{r}_T = \frac{1}{N} \sum_{n=1}^N [\min_{z \in Z_T} \mathcal{L}(\hat{y}(z), y_n)] \tag{10}$$

where  $Z_T$  is a randomly drawn sequence of  $z$  values of length  $T$ . We use mean-squared error as  $\mathcal{L}$ , following convention [2, 1]. A unique set of  $z$  values was drawn for each model, based upon the sampling distribution required by that particular model (e.g., Gaussian for cINN).

The main experimental results are presented in Fig. 3. Measuring  $\hat{r}_T$  as a function of  $T$  yields a much richer characterization of each model’s performance compared to using just  $T = 1$ . In Fig. 3 we see that  $\hat{r}_T$  falls steadily as  $T$  increases, except for the Tandem model which is not stochastic. Therefore  $\hat{r}_T$  quantifies the error one can expect for each model depending upon the computational time/hardware permitted for inference available to a user for their application. Much more interesting is the observation that the performance rank-order of the models also varies with  $T$  for all four tasks. Therefore, the best model for a given task (in terms of  $\hat{r}$ ) also depends upon the time/hardware permitted for inference.

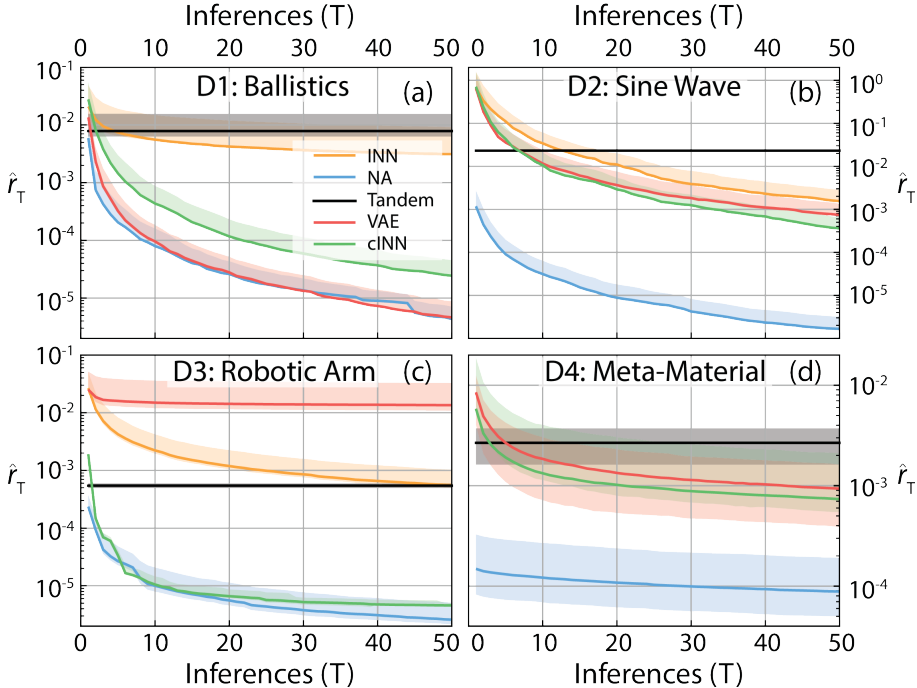


Figure 3: (a-d) Performance on each model for each benchmark task as a function of  $T$ .

### 6.1 Which Models Perform Best?

The NA method almost always yields the most accurate solutions, across both tasks and settings of  $T$ . Especially notable is its large performance advantage on the higher-dimensional meta-material task, suggesting it may be especially effective for similar problems. However, NA has the drawback of significantly greater computational costs than the other models, due to its use of gradient descent. The average inference time for all model/task combinations is shown in Table 2. The remaining models (cVAE, Tandem, INN, cINN) all have relatively comparable inference times. With these computation costs factored in, the Tandem model consistently achieves the best accuracy for time-sensitive applications, where  $T = 1$  (i.e., 1-10 ms). If more than (approximately) 300ms is permitted for processing, then the NA method is always the best choice. This is because all models asymptote within approximately 200 inferences (or, very roughly, 300ms), and the NA method always asymptotes to the lowest error by that time, as shown in Table 3. Between these two boundaries (10ms-300ms) the best model depends upon the particular target task: the cVAE is best for the ballistics problem, while the cINN performs best for the robotic arm.

Table 2: Average Inference time (t) in milliseconds

Dataset	NA	Tandem	cVAE	INN	cINN
D1:Ballistics	1.36	0.31	0.29	0.35	0.78
D2:Sine wave	1.22	0.19	0.19	0.19	0.20
D3:Robotic arm	1.12	0.19	0.31	0.21	0.23
D4:Meta-material	46.10	0.5	0.47	-	0.25

Table 3: Estimated Asymptotic Performance of Each Model ( $\hat{r}_{T=200}$ )

Dataset	NA	Tandem	cVAE	INN	cINN
D1:Ballistics	<b>2.50e-7</b>	7.84e-3	2.80e-7	2.20e-3	1.18e-6
D2:Sine wave	<b>1.33e-7</b>	1.17e-2	4.34e-5	1.24e-4	2.72e-5
D3:Robotic arm	<b>6.61e-7</b>	5.44e-4	1.25e-2	2.12e-4	8.80e-7
D4:Meta-material	<b>6.67e-5</b>	2.53e-3	5.49e-4	-	4.45e-4

## 6.2 Why does the neural-adjoint perform so well?

Notably in Table 3, we see that NA always achieves the lowest asymptotic error as a function of  $T$ , while the other models asymptote at varying levels. Why are the other models limited in their accuracy, even as  $T \rightarrow \infty$ ? One potential explanation is that they do not fully explore  $x$ -space, and thereby miss some accurate solutions. Alternatively, perhaps they can find solutions near all of the global optima, but they cannot accurately localize them (e.g., their estimates are noisy). To answer this question, we visualize the 2-dimensional sinusoid task (D2), on which most of the models perform poorly. Fig. 4 presents a random sample of inverse solutions produced by each model, laid on top of a 2-dimensional error map of  $x$ -space (darker is better). The blue rings indicate the optimal solutions for a target measurement of  $y=-0.3$ . We can see clearly that NA finds highly accurate solutions in each of the globally optimal rings. The cVAE and the cINN seem to find solutions near all of the globally optimal solutions, however they rarely infer perfectly accurate solutions. Therefore both the cVAE and cINN seem to suffer from noisy solutions, rather than inability to find the solutions. Finally, the INN seems unable to search the entire space, in addition to suffering from inaccurate solutions. However, this is a single visualization, representing a single task and a single instance of training the models. We find the relative performance of all models (except NA) varies substantially across tasks *and* the success of their training (which is somewhat random). This suggests that each of these models sometimes suffer from limited exploration of  $x$ -space, and varying accuracy, depending upon the aforementioned factors. These findings are consistent with (e.g., [2]) overall.

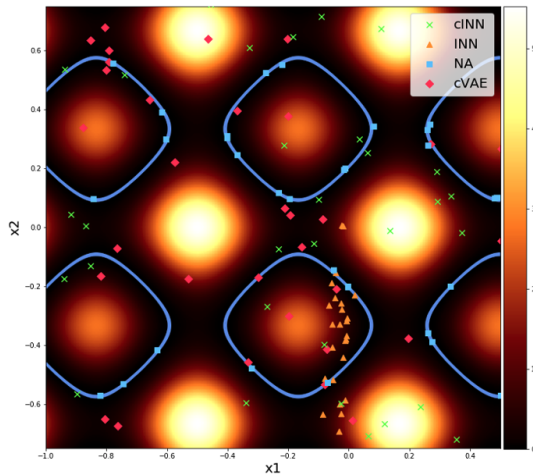


Figure 4: The image axes represent a uniform grid of potential inverse solutions,  $(x_1, x_2)$ , for the 2-dimensional sinusoid problem. The pixel intensity at each  $(x_1, x_2)$  location represents the corresponding simulation error of that solution, if our target measurement is  $y = -0.3$ . The blue rings represent the optimal solutions.

## 7 Conclusions

In this work we presented a large benchmark comparison of five modern deep inverse models, on four benchmark tasks. We propose a new metric,  $r_T$ , that evaluates the error of models as a function of the number of inverse solutions they are permitted to propose, denoted  $T$ . We find that the performance



of inverse models, both in absolute error and in their rank-order, depends strongly on  $T$ , suggesting that  $r_T$  is important to characterize inverse model performance. We also introduce a challenging contemporary inverse problem for meta-material design. Normally, it would be difficult for others to replicate such real-world problems however, we introduce a strategy for creating simple, fast, and sharable *approximate* simulators. Finally, we propose a method called the Neural-Adjoint, which nearly always achieves the lowest error across all tasks and values of  $T$ . Its performance advantage is especially strong for the higher-dimensional meta-material problem, suggesting it is a promising approach to solve such problems.

## Broader Impact

We believe the most proximate impacts of this work will be positive. In particular, higher-dimensional inverse problems like our meta-material problem present a major obstacle to the development of beneficial technologies across many disciplines e.g., in materials, chemistry, and bio-chemistry. The Neural-Adjoint method represents a tool to develop much more accurate inverse designs for these complex problems. Furthermore, the ability to replicate inverse studies for complex problems, as we propose, will also accelerate progress, and enable many researchers to study these problems even if they lack sophisticated simulation equipment or expertise. As with many tools, we also acknowledge that these advances can be used to accelerate the development of technologies that are used for negative purposes, which we believe is the most immediate negative outcome of our work.

## References

- [1] L. Ardizzone, J. Kruse, S. Wirkert, D. Rahner, E. W. Pellegrini, R. S. Klessen, L. Maier-Hein, C. Rother, and U. Köthe, “Analyzing inverse problems with invertible neural networks,” *arXiv preprint arXiv:1808.04730*, 2018.
- [2] J. Kruse, L. Ardizzone, C. Rother, and U. Köthe, “Benchmarking invertible architectures on inverse problems,” ICML, 2019.
- [3] D. P. Kingma and M. Welling, “Auto-encoding variational bayes,” *arXiv preprint arXiv:1312.6114*, 2013.
- [4] D. Liu, Y. Tan, E. Khoram, and Z. Yu, “Training deep neural networks for the inverse design of nanophotonic structures,” *ACS Photonics*, vol. 5, no. 4, pp. 1365–1369, 2018.
- [5] M. I. Jordan and D. E. Rumelhart, “Forward models: Supervised learning with a distal teacher,” *Cognitive science*, vol. 16, no. 3, pp. 307–354, 1992.
- [6] M. P. Bendsoe and N. Kikuchi, “Generating optimal topologies in structural design using a homogenization method,” 1988.
- [7] J. Herskovits, *Advances in Structural Optimization*. Dordrecht: Springer Netherlands, 1995.
- [8] P. Maass, “Deep learning for trivial inverse problems,” in *Compressed Sensing and Its Applications*, pp. 195–209, Springer, 2019.
- [9] J. Song, K. Pang, Y.-Z. Song, T. Xiang, and T. M. Hospedales, “Learning to sketch with shortcut cycle consistency,” in *Proceedings of the IEEE Conference on Computer Vision and Pattern Recognition*, pp. 801–810, 2018.
- [10] J.-Y. Zhu, T. Park, P. Isola, and A. A. Efros, “Unpaired image-to-image translation using cycle-consistent adversarial networks,” in *Proceedings of the IEEE international conference on computer vision*, pp. 2223–2232, 2017.
- [11] L. Pilozi, F. A. Farrelly, G. Marcucci, and C. Conti, “Machine learning inverse problem for topological photonics,” *Communications Physics*, vol. 1, no. 1, pp. 1–7, 2018.
- [12] W. Ma, F. Cheng, Y. Xu, Q. Wen, and Y. Liu, “Probabilistic representation and inverse design of metamaterials based on a deep generative model with semi-supervised learning strategy,” *Advanced Materials*, vol. 31, no. 35, p. 1901111, 2019.
- [13] Y. Kiarashinejad, S. Abdollahramezani, and A. Adibi, “Deep learning approach based on dimensionality reduction for designing electromagnetic nanostructures,” *npj Computational Materials*, vol. 6, no. 1, pp. 1–12, 2020.
- [14] C. M. Bishop, “Mixture density networks,” 1994.
- [15] L. Dinh, J. Sohl-Dickstein, and S. Bengio, “Density estimation using real nvp,” *arXiv preprint arXiv:1605.08803*, 2016.

- [16] E. G. Tabak, E. Vanden-Eijnden, *et al.*, “Density estimation by dual ascent of the log-likelihood,” *Communications in Mathematical Sciences*, vol. 8, no. 1, pp. 217–233, 2010.
- [17] D. P. Kingma, T. Salimans, R. Jozefowicz, X. Chen, I. Sutskever, and M. Welling, “Improved variational inference with inverse autoregressive flow,” in *Advances in neural information processing systems*, pp. 4743–4751, 2016.
- [18] M. Germain, K. Gregor, I. Murray, and H. Larochelle, “Made: Masked autoencoder for distribution estimation,” in *International Conference on Machine Learning*, pp. 881–889, 2015.
- [19] B. Uria, M.-A. Côté, K. Gregor, I. Murray, and H. Larochelle, “Neural autoregressive distribution estimation,” *The Journal of Machine Learning Research*, vol. 17, no. 1, pp. 7184–7220, 2016.
- [20] L. Dinh, D. Krueger, and Y. Bengio, “Nice: Non-linear independent components estimation,” *arXiv preprint arXiv:1410.8516*, 2014.
- [21] J. Peurifoy, Y. Shen, L. Jing, Y. Yang, F. Cano-Renteria, B. G. DeLacy, J. D. Joannopoulos, M. Tegmark, and M. Soljačić, “Nanophotonic particle simulation and inverse design using artificial neural networks,” *Science advances*, vol. 4, no. 6, p. eaar4206, 2018.
- [22] D. P. Kingma and J. Ba, “Adam: A method for stochastic optimization,” *arXiv preprint arXiv:1412.6980*, 2014.
- [23] A. Gretton, K. M. Borgwardt, M. J. Rasch, B. Schölkopf, and A. Smola, “A kernel two-sample test,” *Journal of Machine Learning Research*, vol. 13, no. Mar, pp. 723–773, 2012.
- [24] C. C. Nadell, B. Huang, J. M. Malof, and W. J. Padilla, “Deep learning for accelerated all-dielectric metasurface design,” *Optics express*, vol. 27, no. 20, pp. 27523–27535, 2019.
- [25] M. H. Tahersima, K. Kojima, T. Koike-Akino, D. Jha, B. Wang, C. Lin, and K. Parsons, “Deep neural network inverse design of integrated nanophotonic devices,” *arXiv preprint arXiv:1809.03555*, 2018.
- [26] Z. Liu, D. Zhu, S. P. Rodrigues, K.-T. Lee, and W. Cai, “Generative model for the inverse design of metasurfaces,” *Nano letters*, vol. 18, no. 10, pp. 6570–6576, 2018.